

# Effective photon spectra for the photon colliders

I.F. Ginzburg<sup>1,a</sup>, G.L. Kotkin<sup>2,b</sup>

<sup>1</sup> Institute of Mathematics, Prosp. Acad. Koptyug 4, 630090 Novosibirsk, Russia

<sup>2</sup> Novosibirsk State University, Ul. Pirogova 2, 630090 Novosibirsk, Russia

Received: 14 September 1999 / Published online: 17 February 2000 – © Springer-Verlag 2000

**Abstract.** The luminosity distribution in the effective  $\gamma\gamma$  mass at a photon collider usually has two peaks which are well separated: a high energy peak with mean energy spread about 5–7% and a wide low energy peak. The low energy peak strongly depends on the details of the design and is unsuitable for the study of new physics phenomena. We find a simple approximate form for the spectra of *colliding photons* for  $\gamma\gamma$  and  $e\gamma$  colliders, whose convolution describes the high energy luminosity peak with a good accuracy in most of the essential preferable region of the parameters.

## 1 Introduction

The photon colliders ( $\gamma\gamma$  and  $e\gamma$ ) were proposed and discussed in detail in [1]. Forthcoming papers [2,3] present some new details of the design and analysis of some effects involved in a conversion.

In the basic scheme two electron beams leave the final focus system and travel towards the interaction point (IP). At the conversion point (CP) at the distance  $b \sim 1\text{--}10$  mm before IP they collide with focused laser beams. The Compton scattering of a laser photon off an electron produces a high energy photon. The longitudinal motion of this photon originates from that of the electron, so these photons follow the trajectories of the electrons (to the IP) with additional an angular spread  $\sim 1/\gamma$ . With reasonable laser parameters, one can “convert” most of the electrons into high energy photons. Without taking into account rescattering of the electrons on the next laser photons, the total  $\gamma\gamma$  and  $e\gamma$  luminosities are  $\mathcal{L}_{\gamma\gamma}^0 = k^2 \mathcal{L}_{ee}$  and  $\mathcal{L}_{e\gamma}^0 = k \mathcal{L}_{ee}$ , where  $k$  is the conversion coefficient and  $\mathcal{L}_{ee}$  is the geometrical luminosity of the basic  $ee$  collisions, which can be made much larger than the luminosity of the basic  $e^+e^-$  collider. Below we assume distances  $b$  and the form of the electron beams to be identical for the two beams.

Let the energy of the initial electron, laser photon and high energy photon be  $E$ ,  $\omega_0$  and  $\omega$ . We as usual define

$$x = \frac{4E\omega_0}{m_e^2}, \quad y = \frac{\omega}{E} \leq y_m = \frac{x}{x+1}. \quad (1)$$

The quality of the photon spectra is better for higher  $x$ . However, at  $x > 2(1+2^{1/2}) \approx 4.8$  the high energy photons can disappear via the production of an  $e^+e^-$  pair due to

collision with a following laser photon. That is why the preferable conversion is at  $x = 4\text{--}5$ .

The energies of the colliding photons  $\omega_i = y_i E$  can be determined for each event by measuring the total energy of the produced system  $\omega_1 + \omega_2$  and its total (longitudinal) momentum  $\omega_1 - \omega_2$ . We discuss in more detail the main area for study of new physics – *the high energy region* where the energies of both photons are large enough. For definiteness we consider the photon energy region  $(y_m/2) < y_i < y_m$  and additionally demand that no photons with lower energy contribute to the entire distribution over the effective mass of the  $\gamma\gamma$  system  $2zE$  or its total energy  $YE$ :

$$\frac{y_m}{2} < y_1, y_2 < y_m \Rightarrow \left( \frac{y_m}{\sqrt{2}} < z = \sqrt{y_1 y_2} < y_m \right), \\ (1.5y_m < Y = y_1 + y_2 < 2y_m). \quad (2)$$

In the interesting cases this choice covers the high energy peak in the luminosity since the photon spectra are concentrated in the more narrow regions near  $y_m$ .

The growth of the distance  $b$  between IP and CP is accompanied by two phenomena. First, high energy collisions become more monochromatic. The high energy part of the luminosity is concentrated in a relatively narrow peak which is well separated from the additional low energy peak. This separation becomes stronger at higher  $x$  and  $b$  values. Second, the luminosity in the high energy region decreases (relatively slowly at small  $b$  and as  $b^{-2}$  at large  $b$ ). Only the high energy peak is the area for study of the new physics phenomena. The low energy peak is the source of background in these studies. The separation between the peaks is very useful to eliminate the background from the data. Therefore, some intermediate value of  $b$  provides the best conditions for the study of new physics.

<sup>a</sup> e-mail: ginzburg@math.nsc.ru

<sup>b</sup> e-mail: kotkin@math.nsc.ru

To begin, let us discuss the spectra neglecting rescattering. At  $b = 0$  the  $\gamma\gamma$  luminosity distribution is a simple convolution of two photon spectra of separate photons. At  $b \neq 0$  the luminosity distribution is a more complicated convolution of the above photon spectra with some factor depending on  $b$  and on the form of the initial electron beams. With the growth of the conversion coefficient the effect of rescattering of the electrons on the laser photons enhances and make this distribution dependent on the details of the design (mainly, in the low energy part).

In this paper we continue the discussion from [1] about the main parameters of scheme which are preferable for the  $\gamma\gamma$  and  $e\gamma$  colliders for elliptic electron beams. We find the universal description of the high energy peak in this preferable region of parameters. It allows us to obtain the remarkable approximate form of the spectra of *colliding photons*, whose simple convolution describes the high energy luminosity peak with a reasonable accuracy.

## 2 Luminosity distribution without rescattering. Elliptic electron beams

The high energy peak in the luminosity is described mainly by a single collision of an electron with a laser photon; this part of the distribution depends on the form of the initial beams only. Therefore, we start with a detailed discussion of the effects from a single electron and laser photon collision. First, we review some basic points from [1].

The scattering angle of a produced photon  $\theta$  is related to its energy by

$$\theta = \frac{g(x, y)}{\gamma}, \quad g(x, y) = \sqrt{\frac{x}{y} - x - 1}, \quad \gamma = \frac{m_e}{E}. \quad (3)$$

Let the mean helicities of initial electron, laser photon and high energy photon be  $\lambda_e/2$ ,  $P_\ell$  and  $\xi_2$ . The energy spectrum of the produced photons is ( $N$  is a normalization factor)

$$F(x, y) = N \left[ \frac{1}{1-y} - y + (2r-1)^2 - \lambda_e P_\ell x r (2r-1)(2-y) \right], \quad (4)$$

$$r = \frac{y}{x(1-y)}.$$

At  $\lambda_e P_\ell = -1$  and  $x > 1$  this spectrum has a sharp peak at high energy, which becomes even sharper with growing  $x$ .

The spectrum is sharper when  $-\lambda_e P_\ell$  is larger. Below we mainly present the values from the actual projects:  $\lambda_e = 0.85$ ,  $P_\ell = -1$ .

The degree of circular polarization of the high energy photon is

$$\langle \xi_2 \rangle = N \frac{\lambda_e x r [1 + (1-y)(2r-1)^2] - P_\ell (2r-1) \left[ \frac{1}{1-y} + 1 - y \right]}{F(x, y)}. \quad (5)$$

The photons with a lower energy have a higher production angle (3). With the growth of  $b$ , these photons spread more

and more, and they collide only rarely. Therefore, with the growth of  $b$ , photon collisions become more monochromatic, only high energy photons taking part in these collisions and the low energy part of the total luminosity being rejected (here photons on average are almost non-polarized).

This effect was studied in [1] for the gaussian round electron bunches. However, the incident electron beams are expected to be of an elliptic form with a large enough ellipticity.

Let the initial electron beams be of the gaussian elliptic form with vertical and horizontal sizes  $\sigma_{ye}$  and  $\sigma_{xe}$  at the IP (calculated for the case without conversion). The discussed phenomena are described by a reduced distance between conversion and collision points  $\rho$  and the aspect ratio  $A$ :

$$\rho^2 = \left( \frac{b}{\gamma \sigma_{xe}} \right)^2 + \left( \frac{b}{\gamma \sigma_{ye}} \right)^2, \quad A = \frac{\sigma_{xe}}{\sigma_{ye}}. \quad (6)$$

The luminosity distributions in this case can be calculated by the same approach as was used in [1].

The distribution of the photons colliding with opposite electrons at the  $e\gamma$  collider is

$$\frac{d\mathcal{L}_{e\gamma}}{dy} = \int \frac{d\phi}{2\pi} F(x, y) \times \exp \left[ -\frac{\rho^2 g^2(x, y)}{4(1+A^2)} (A^2 \cos^2 \phi + \sin^2 \phi) \right]. \quad (7)$$

For the round beams ( $A = 1$ ) we have in the exponent  $\rho^2 g^2(x, y)/8$ .

The distribution of the colliding photons over their energies at the  $\gamma\gamma$  collider is

$$\frac{d^2\mathcal{L}_{\gamma\gamma}}{dy_1 dy_2} = \int \frac{d\phi_1 d\phi_2}{(2\pi)^2} F(x, y_1) F(x, y_2) \times \exp \left[ -\frac{\rho^2 \Psi}{4(1+A^2)} \right],$$

$$\Psi = A^2 [g(x, y_1) \cos \phi_1 + g(x, y_2) \cos \phi_2]^2 + [g(x, y_1) \sin \phi_1 + g(x, y_2) \sin \phi_2]^2. \quad (8)$$

For the round beams ( $A = 1$ ) one can perform the integrations over  $\phi_i$  in analytical form. This results in the equation from [1] with the Bessel function of an imaginary argument,  $I_0(v^2)$ ,

$$\frac{d^2\mathcal{L}_{\gamma\gamma}}{dy_1 dy_2} = F(x, y_1) F(x, y_2) \times \exp \left[ -\frac{\rho^2}{8} (g^2(x, y_1) + g^2(x, y_2)) \right] I_0(v),$$

$$v^2 = \frac{\rho^2}{4} g(x, y_1) g(x, y_2). \quad (9)$$

We have numerically analyzed the high energy part of the luminosity (in the region (2)),  $\mathcal{L}^h$ , as a function of  $\rho^2$  and  $A$  at  $2 < x < 5$ ,  $-\lambda_e P_\ell \geq 0$ . (We use this notation for both the total luminosity integrated over the region (2) and the differential distributions.)

**Table 1.** The ratio of the high energy luminosity  $\mathcal{L}^h$  to the total luminosity  $\mathcal{L}_{\gamma\gamma}^0$  at some values of the parameters

$\lambda_e P_\ell$	$\rho = 0$ , any $A$		$\rho = 1$ , $A \geq 1.5$	
	-0.85	0	-0.85	0
$x = 4.8$	0.35	0.25	0.28	0.19
$x = 2$	0.29	0.19	0.25	0.16

The growth of  $\rho$  results both in a better form of the luminosity distribution and a reduction of the luminosity. We find that the luminosity  $\mathcal{L}^h$  depends only weakly on the aspect ratio  $A$  at  $A > 1.5$  and  $\rho^2 < 1.3$ . At  $\rho^2 \leq 1$  this dependence is weak at all values of  $A$  (including  $A = 1$ ). For  $\lambda_e P_\ell = -0.85$ , the luminosity  $\mathcal{L}^h$  at  $\rho = 1$  contains a large enough fraction from the high energy part of the luminosity given at  $\rho = 0$ . For the unpolarized case ( $\lambda_e P_\ell = 0$ ) both this fraction is smaller and the high energy peak is separated weakly from the low energy one. Some of these statements can be seen from Table 1, where we show the ratio of the high energy luminosity  $\mathcal{L}^h$  to the total luminosity  $\mathcal{L}_{\gamma\gamma}^0$  for some values of the parameters.

It seems unreasonable to use the lowest part of the total luminosity rather than that obtained at  $\rho = 1$ .

To have a more detailed picture for the simulation, we study the luminosity distribution in the relative values of the effective mass  $z = W/(2E)$  and the total energy  $Y = \mathcal{E}/E$  of the pair of colliding photons (2). Their typical forms for different values of the aspect ratio  $A$  are shown in Figs. 1 and 2.

A numerical study of these distributions shows that its high energy part is practically the same for all values  $A > 1.5$  at fixed  $\rho^2 < 1.3$  (with a small difference near the lower part of the peak). The luminosity within the high energy peak for round beams ( $A = 1$ ) is slightly lower than that for the elliptic beams. This difference is about 5% in the main part of the region below the peak. At  $\rho^2 = 1$  this difference is small for all  $A$ . At  $\rho^2 > 0.5$  the high energy part of the luminosity has the form of a narrow enough peak. This peak is not so sharp at lower  $x$  and it is even less sharp at  $\lambda_e P_\ell = 0$ .

With the growth of the aspect ratio  $A$  the entire distributions acquire low energy tails (as compared with round beams) originating from the collisions of low energy photons scattered near the horizontal direction with the opposite high energy photons scattered in the vertical direction. This tail is added to that from the rescatterings and is not of much interest in the discussion of the high energy peak. At higher  $\rho$  and  $A$  this effect becomes more essential in the region of the peak.

As a result, the preferable region of the parameters for the photon colliders is

$$5 > x > 2, \quad -\lambda_e P_\ell \geq 0.5, \quad \rho^2 < 1.3. \quad (10)$$

Additionally, here the high energy peaks in the  $\gamma\gamma$  and  $e\gamma$  luminosities are described by one parameter,  $\rho$ , and are practically independent of  $A > 1.5$ .

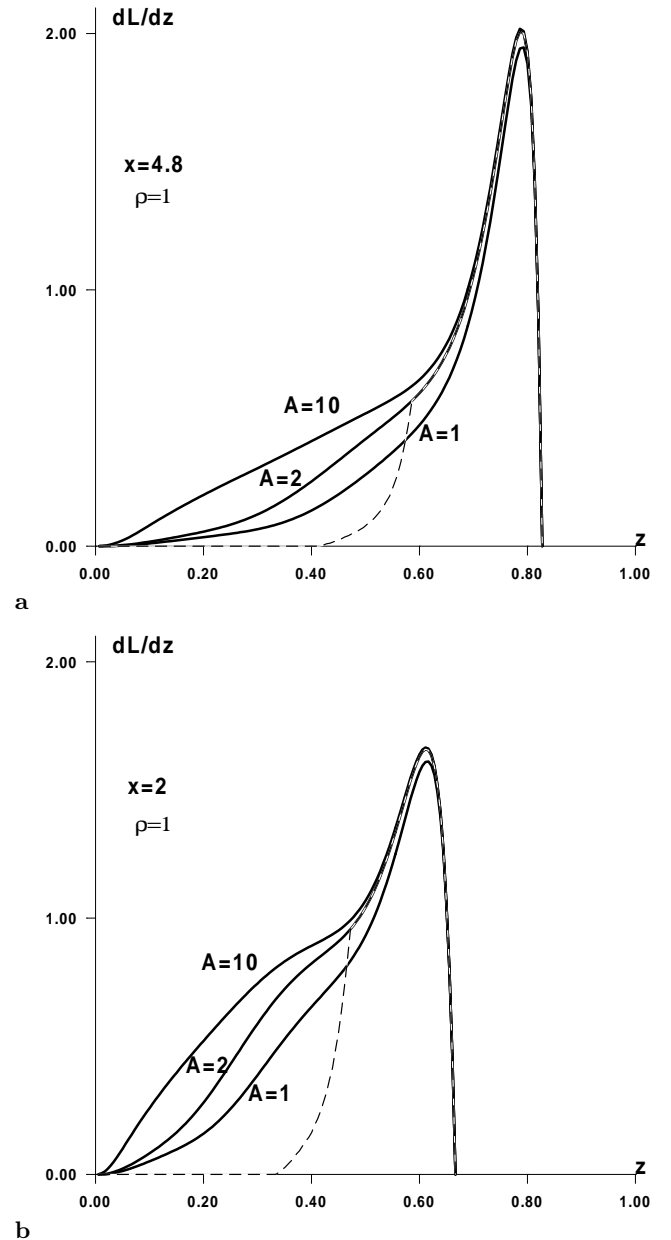


**Fig. 1a,b.** The luminosity distributions in the effective mass of the  $\gamma\gamma$  system at  $\lambda_e P_\ell = -0.85$ . The dashed line presents this distribution for  $y_i > y_m/2$  at  $A = 2$

### 3 Rescattering contribution to the spectra. Qualitative description

The rescattering of electrons on the following laser photons produces new high energy photons (*secondary photons*) which modify the luminosity distribution mainly in the low energy part. The detailed form of the additional components of the luminosity distribution strongly depends on the conversion coefficient and other details of the design. That is why we here present only a qualitative discussion with some simple examples.

Let us enumerate the differences in properties of secondary photons from those from the first collision (we will

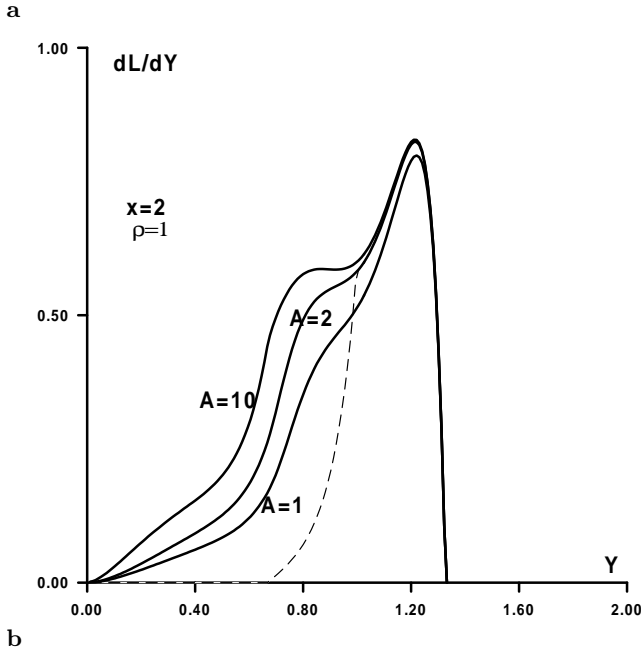
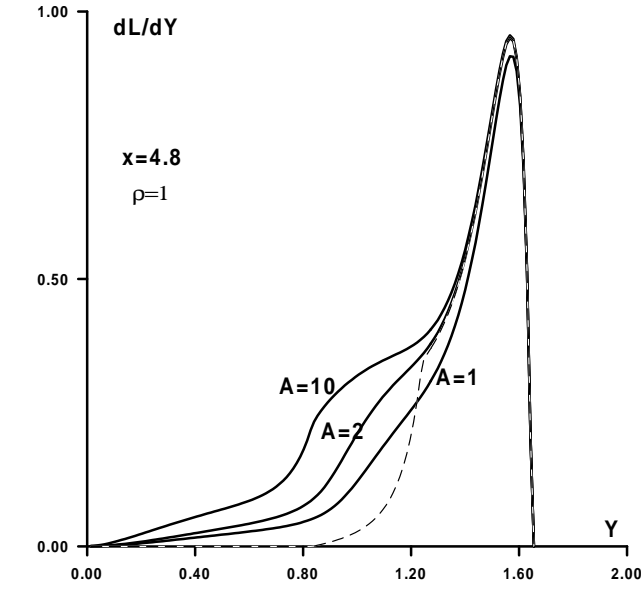


**Fig. 2a,b.** The luminosity distributions in the total energy of the  $\gamma\gamma$  system at  $\lambda_e P_\ell = -0.85$ . The dashed line presents this distribution for  $y_i > y_m/2$  at  $A = 2$

denote them as *primary photons*).

- (1) The energy of the secondary photons is lower than that of the primary photons.
- (2) There is no definite relation between the energy and the production angle like (3).
- (3) The mean polarization of the secondary photons is practically zero.

Figure 3 presents a typical energy spectrum of photons with only one rescattering at the conversion coefficient  $k = 1$ . The dashed line represents the fraction of secondary photons. Let us explain some features of this spectrum.

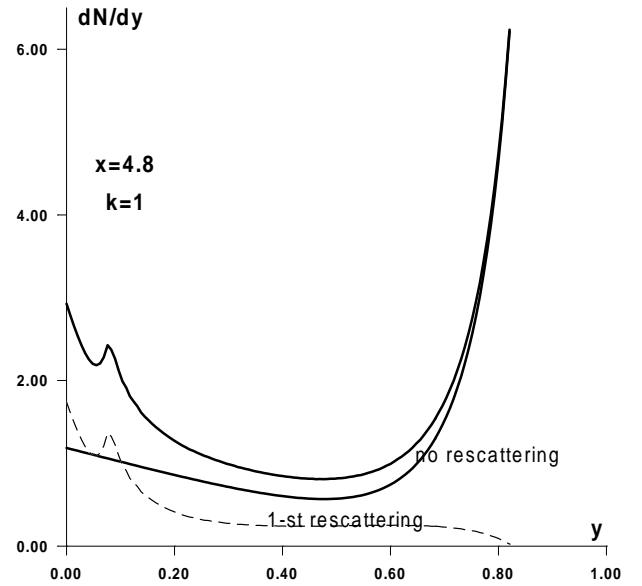


**Fig. 3.** The energy spectrum of photons with one rescattering,  $\lambda_e P_\ell = -0.85$

The main fraction of the electrons after the first scattering has an energy which corresponds to the peak in the produced photon spectra,  $E_e \approx E - \omega_m = E/(x + 1)$ . For the next collision  $x \rightarrow x/(x + 1)$ . Therefore, the additional energy peak in the photon spectrum caused by secondary photons from the first rescattering is at the photon energy  $\sim y_m/(2x + 1)$ ; it is much lower than  $y_m E$  for  $x > 2$ . The subsequent rescatterings add more soft photons. Besides, the primary photon spectrum (4) is concentrated near its high energy boundary. So, the fraction of scattered electrons with an energy close to  $E$  is small, and the effect of rescattering in the high energy part on the entire photon spectrum is also small. In the subsequent rescatterings such peaks become smooth. The well-known result is a large peak near  $y = 0$ . Note also that the secondary photons on average are nonpolarized.

The shape of the additional contribution of secondary photons to the luminosity distributions (secondary–secondary and primary–secondary) depends on  $k$ ,  $\rho$  and  $A$ . Nevertheless, the different simulations show common features (see [2,3]).

At  $\rho^2 \geq 0.5$ ,  $k \lesssim 1$ , the luminosity distribution has two well separated peaks: a *high energy peak* (mainly from *primary photons*) and a *wide low energy peak* (mainly from *secondary photons*). Photons in the high energy peak have a high degree of polarization, the mean polarization of photons in the low energy peak is close to 0. At smaller  $x$  or  $-\lambda_e P_\ell$  this separation of peaks becomes less definite and the mean photon polarization becomes less than that given by (5).

With a good separation of the peaks, the backgrounds from the low energy peak could be eliminated relatively easily in many problems.

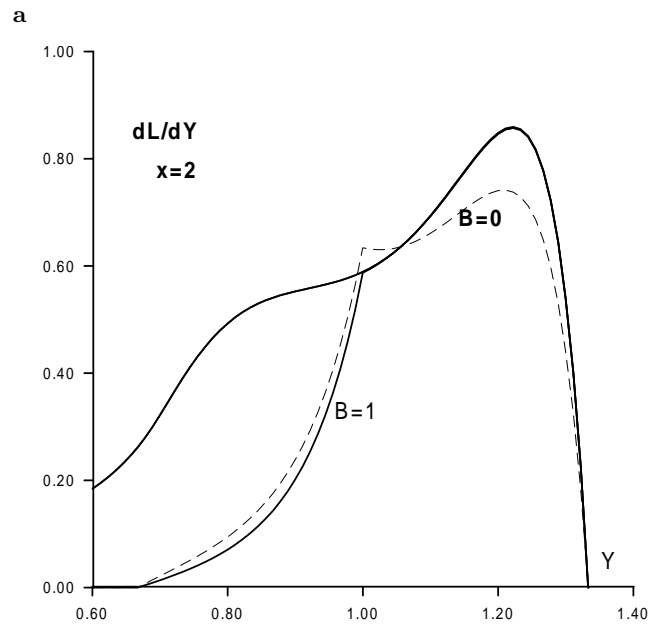
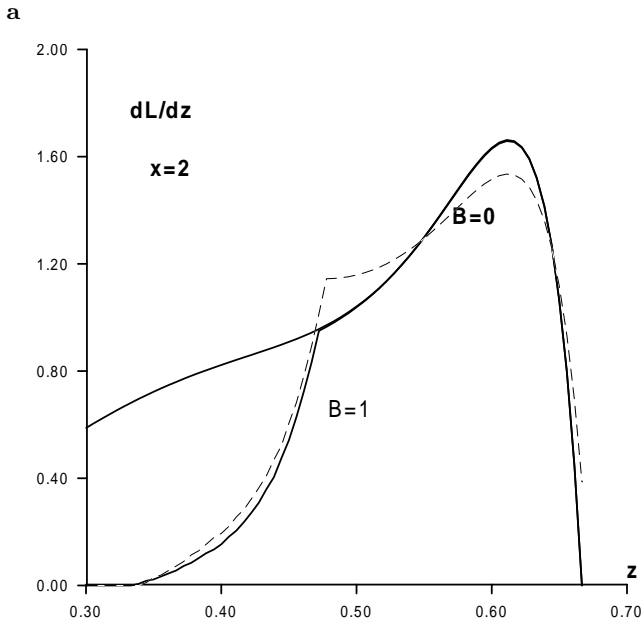
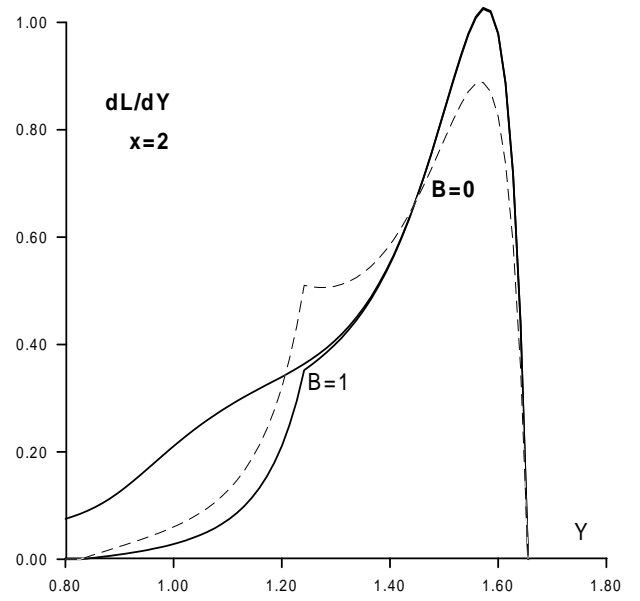
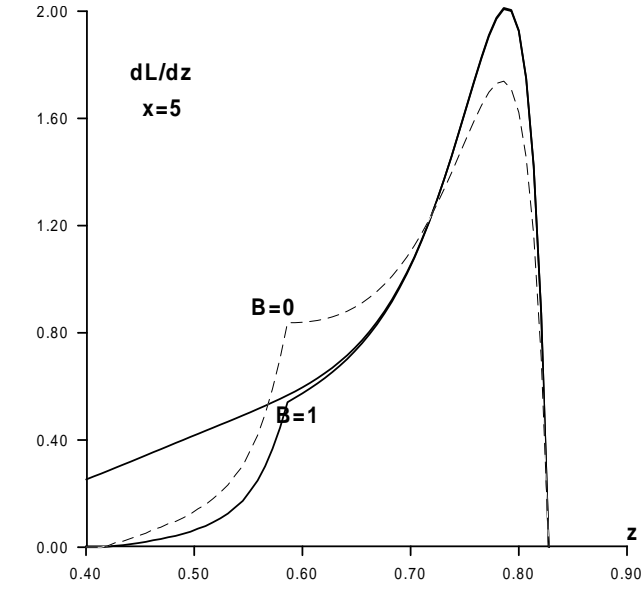


**Fig. 4a,b.** The precise luminosity distribution in the effective mass of the  $\gamma\gamma$  system without rescattering at  $A = 2$  and with approximation (11)–(13). The dashed line is for the “simplified” spectra

**Fig. 5a,b.** The precise luminosity distribution in the total energy of the  $\gamma\gamma$  system without rescattering at  $A = 2$  and with approximation (11)–(13). The dashed line is for the “simplified” spectra

### 4 Approximation

The previous discussion shows us that there are chances to construct an approximation for photon spectra which would describe the high energy peak in a simple and universal way. We were searching for an approximation in which the high energy peak in the  $\gamma\gamma$  luminosity would be given by a simple convolution of the form

$$\frac{d^2\mathcal{L}}{dy_1 dy_2} = F_a(x, y_1, \rho^2) F_a(x, y_2, \rho^2), \quad (11)$$

instead of a complex integration (8) (independent of the aspect ratio  $A$ ).

We tested different forms of effective photon spectra. Taking into account the form of angular spread of the separate beam, we consider a test function for the high energy peak in the form

$$F_a(x, y, \rho^2) = \begin{cases} F(x, y) \exp[-B\rho^2 g^2(x, y)/8] & \text{at } y > y_m/2, \\ 0 & \text{at } y < y_m/2, \end{cases} \quad (12)$$

where the coefficient  $B$  is varied.

A good fit for the high energy peak at  $2 < x < 5$ ,  $\rho^2 < 1.3$ ,  $A > 1.5$  is given by the values

$$\begin{aligned} B &= 1 && \text{for the } \gamma\gamma \text{ collider,} \\ B &= 0.7 && \text{for } e\gamma \text{ collider.} \end{aligned} \quad (13)$$

In particular, we have for the  $\gamma\gamma$  collisions

$$F_a(x, y, \rho^2) = \begin{cases} F(x, y) \exp \left[ -\rho^2 \left( \frac{x}{y} - x - 1 \right) / 8 \right] & \text{at } y > y_m/2, \\ 0 & \text{at } y < y_m/2. \end{cases} \quad (14)$$

Typically  $\rho = 1$ .

The curves in Figs. 4 and 5 show the accuracy of this approximation for the distributions in both the effective  $\gamma\gamma$  mass  $z = (y_1 y_2)^{1/2}$  and the total photon energy  $Y = y_1 + y_2$  at  $\lambda_e P_\ell = -0.85$ . These curves show the excellent quality of our approximation. It is difficult to distinguish the exact curve and the approximation within the approximation region.

Sometimes the “simplified” approximating spectra are used in which this spectrum coincides with that in the photon beam without angular spread [4]. It can be obtained from our (12) at  $B = 0$  and with adding of some factor  $G(\rho)$  to get the same total luminosity in the high energy peak ( $G^2(\rho) = \mathcal{L}(\rho)/\mathcal{L}(\rho = 0)$ ). The corresponding curves are shown in Figs. 4 and 5 by dashed lines ( $B = 0$ ). It is seen that in this approximation the luminosity spectra look less monochromatic than they are in reality.

Note that the approximation (13) for the  $\gamma\gamma$  collision can be obtained from (9) if the Bessel functions  $I_0(v^2)$  are replaced by unity. Figures 4 and 5 show that our approximation coincide practically with precise distributions within the high energy peak for the elliptic beams ( $A \geq 1.5$ ). Therefore, the difference between the curves for  $A = 1$  and  $A = 2$  in Figs. 1 and 2 in the region (2) is caused by the Bessel function factor.

Using the “precise” equation (8) instead of our approximation is only a minor improvement. The difference between the approximation and the “precise” formula is usually smaller than the effect of the rescatterings.

## 5 Results

Let us enumerate the main results.

- (1) The variable  $\rho$  (6) is a good variable for the description of the high energy peak in the spectral luminosity, independent of the aspect ratio  $A$  at  $A > 1.5$ ,  $\rho^2 < 1.3$ ,  $2 < x < 5$ ,  $\lambda_e P_\ell < 0$ .
- (2) At  $\rho \sim 1$  and suitable polarizations of the initial beams the high energy peak in the luminosity is separated well from the low energy peak. This separation can be destroyed by using a large conversion coefficient or (and) values  $x \approx 1$  or  $\lambda_e P_\ell > 0$ .
- (3) To discuss future experiments with the photon collider with a good enough accuracy, one can use the simple approximation (11)–(13) at  $\rho = 1$  instead of details of the simulation of conversion and collision. In this approximation the details of the design are inessential. A possible decreasing of  $\rho^2$  to the value 0.5 can also be considered.
- (4) The numbers describing the luminosity of the photon collider correspond to the discussed high energy peak only.

*Acknowledgements.* We are grateful to G. Jikia, V.G. Serbo and V.I. Telnov for useful discussions. This work was supported by grant RFBR 99-02-17211 and a grant of Sankt-Petersburg Center of Fundamental Sciences.

## References

1. I.F. Ginzburg, G.L. Kotkin, V.G. Serbo, V.I. Telnov, Nucl. Instr. Methods **205**, 47 (1983); I.F. Ginzburg, G.L. Kotkin, S.L. Panfil, V.G. Serbo, V.I. Telnov, Nucl. Instr. Meth. **219**, 5 (1984)
2. See e.g. Proceedings Workshop on  $\gamma\gamma$  Colliders, Nucl. Instr. Meth. A **355**, 1 (1995); Zeroth-order design report for the NLC, SLAC Report 474 (1996); TESLA, SBLC conceptual design report, DESY 97-048, ECFA-97-182 (1997); R. Brinkmann et al., Nucl. Instr. Meth. A **406**, 13 (1998); I. Watanabe et al., KEK Report 97-17
3. V.I. Telnov, hep-ex/9810019 and references therein
4. V.I. Telnov, private communication